

# Journal of Materials Chemistry C

Accepted Manuscript



This is an *Accepted Manuscript*, which has been through the Royal Society of Chemistry peer review process and has been accepted for publication.

*Accepted Manuscripts* are published online shortly after acceptance, before technical editing, formatting and proof reading. Using this free service, authors can make their results available to the community, in citable form, before we publish the edited article. We will replace this *Accepted Manuscript* with the edited and formatted *Advance Article* as soon as it is available.

You can find more information about *Accepted Manuscripts* in the [Information for Authors](#).

Please note that technical editing may introduce minor changes to the text and/or graphics, which may alter content. The journal's standard [Terms & Conditions](#) and the [Ethical guidelines](#) still apply. In no event shall the Royal Society of Chemistry be held responsible for any errors or omissions in this *Accepted Manuscript* or any consequences arising from the use of any information it contains.

## PAPER

# Lowering Contact Resistance by SWCNT-Al Bilayer Electrodes in Solution Processable Metal-Oxide Thin Film Transistor

Cite this: DOI: 10.1039/x0xx00000x

Received 00th January 2012,  
Accepted 00th January 2012

DOI: 10.1039/x0xx00000x

[www.rsc.org/](http://www.rsc.org/)

Su Jeong Lee,<sup>‡a</sup> Tae Il Lee,<sup>‡b</sup> Jee Ho Park,<sup>a</sup> Il-Kwon Oh,<sup>c</sup> Hyungjun Kim,<sup>c</sup> Jung Han Kim,<sup>d</sup> Chul-Hong Kim,<sup>d</sup> Gee Sung Chae,<sup>d</sup> Hong Koo Baik,<sup>a</sup> and Jae-Min Myoung<sup>\*a</sup>

We introduced a single-wall carbon nanotube (SWCNT)-Al bilayer as electrodes for the high-performance solution processable thin film transistor (TFT). The contact resistance was systematically lowered by inserting an Al layer between the SWCNTs and the indium-oxide (In<sub>2</sub>O<sub>3</sub>). The performance of the device was considerably enhanced by adopting the SWCNT-Al bilayer electrodes, thanks to the enlargement of the electrodes contact area and to the formation of an Ohmic contact between the electrodes and the semiconductor. The TFT using the SWCNT-Al bilayer electrodes show a threshold voltage of 0.45 V, a mobility of 4.50 cm<sup>2</sup>/V·s and an *I*<sub>on</sub>/*I*<sub>off</sub> of 6.86 × 10<sup>5</sup>.

## Introduction

A low cost, solution processable, metal-oxide based thin film transistor (TFT) has been recently studied and developed as an alternative to the conventional high cost vacuum processes.<sup>1-7</sup> Especially, studies focused on manufacturing flexible and transparent electronic components by using the solution process are very important for future electronics. Among various electronic components, an electrical conductor presenting both flexibility and transparency properties has been considered very attractive.<sup>8-15</sup> This electrical conductor should be designed in order to present a nanowire or nanotube network structure.<sup>16</sup> Recently, An Ag nanowire network film has been found as the best flexible and transparent electrodes, due to its high conductivity and transparency (at 85% in visible light).<sup>12,13</sup> However, since Ag nanowires are vulnerable to heat, it is difficult to exploit this material for the industrial production of devices. If Ag nanowires are exposed to air or to temperature above 200 °C, they are partially oxidized or melted. During melting, thermal aggregation usually occurs. Further, the cross-linked Ag nanowires turn into individual hemi-spherical Ag particles on the substrate, causing not only a rapid increase in the sheet resistance but also a degradation of the electrical characteristics typical of the devices.<sup>17-19</sup> In contrast, single-wall carbon nanotubes (SWCNTs) are oxidized at temperatures above 350 °C, and present high flexibility, excellent chemical

inertness, and outstanding mechanical, electrical and optical properties.<sup>20-23</sup>

Besides electrical conductivity and transparency, the contact resistance between the electrodes and the solution processable metal-oxide semiconducting layer is an important factor affecting the electrical performance of a device. Unfortunately, the majority of electrically conductive nanowires or nanotubes show a high work function, whereas the solution processable metal oxides are basically n-type semiconductors; thus the electrical contact resistance between the two solution processable materials is high.<sup>24,25</sup>

In order to solve this electrical contact issue, we proposed an energy-band-engineered ultra-thin metal layer insertion between the SWCNTs and the solution processable transition metal oxide channel layer for the first time. Experimentally, we chose to employ an ultra-thin aluminum (Al) layer between the SWCNTs and the n-type metal oxide semiconductor junction. Lowering the contact resistance is made possible through two different mechanisms.

The first is geometric: a continuous Al film can increase the effective contact area with the metal oxide film compared to the porous SWCNTs. The second is based on the nature of the materials: the electronic barrier between the n-type metal oxide and the SWCNTs can be reduced by inserting an Al layer, which generally forms a good electrical Ohmic contact with the metal oxide because of its low work function, which is close

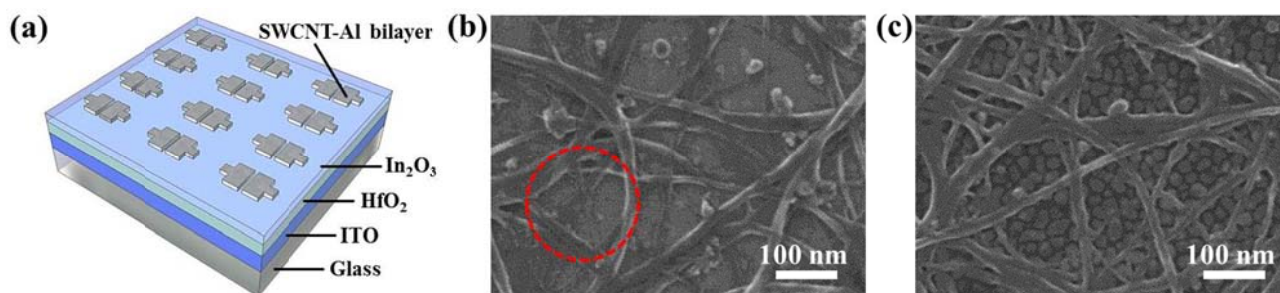


Fig. 1 (a) Schematic diagram of SWCNT-Al bilayer electrode TFT. SEM images of (b) SWCNT layer and (c) SWCNT/7 nm-thick Al bilayer on  $\text{In}_2\text{O}_3$  channel layer.

near to the Fermi energy level of the metal oxide. We determined experimentally the effect of the Al inter layer on the reduction of the contact resistance between the SWCNTs and a solution processed indium-oxide ( $\text{In}_2\text{O}_3$ ) thin film.

## Experimental

Fig. 1a shows a schematic diagram of a bottom gate type TFT with a staggered structure. Indium tin oxide (ITO) films, having a thickness of 100 nm, were deposited on glass substrates by DC magnetron sputtering from an ITO target composed of 90 wt% indium oxide ( $\text{In}_2\text{O}_3$ ) and 10 wt% tin oxide ( $\text{SnO}_2$ ). ITO deposited glass substrate was cleaned using acetone, isopropyl alcohol (IPA), deionized (DI) water by an ultrasonic bath for 15 min, respectively. For the deposition of the hafnium oxide ( $\text{HfO}_2$ ) on the ITO/glass substrate, a commercial atomic layer deposition (ALD) method was used. To obtain a sufficiently high vapor pressure,  $\text{HfCl}_4$  precursors were evaporated at 170 °C in a stainless-steel bubbler. Ar gas was used not only to carry the vapor precursors into the reaction chamber but also to purge the excess gas molecules and byproducts between reactant exposure step and each precursor. The substrate temperature was maintained at 250 °C for the whole ALD process. To prepare the  $\text{In}_2\text{O}_3$  solution, 0.1 M indium nitrate hydrate [ $\text{In}(\text{NO}_3)_3 \cdot x\text{H}_2\text{O}$ ] was vigorously stirred for 24 h in DI water and eventually dissolved. The  $\text{In}_2\text{O}_3$  solution was filtered through polytetrafluoroethylene (PTFE) syringe filters having 0.2  $\mu\text{m}$  pores, spin-coated at 3000 rpm for 20 s onto a  $\text{HfO}_2$ /ITO/glass substrate, and annealed at 250 °C for 1.5 h.<sup>26</sup>

The SWCNT-Al bilayer structure was employed for the source and drain electrodes. Al was deposited by e-beam evaporator at room temperature and the film thicknesses were 5, 7 and 9 nm, respectively. The SWCNTs made by the arc discharge method were provided from Nano Solution Co. Ltd. (SA-210). The SWCNTs were well dispersed in DI water with the help of a surfactant (sodium dodecyl sulfate). The SWCNT film was deposited on the Al contact layer using a spray coating at 115 °C. Afterward, the films were rinsed with DI water for 5 minutes in order to completely remove the surfactant. Finally, the source and drain electrodes were defined by using a photolithography and lift-off process.<sup>25</sup>

The thickness of the  $\text{HfO}_2$ ,  $\text{In}_2\text{O}_3$ , Al films were measured by a

spectroscopic ellipsometry (SEMG-Vis 1000, Nano View). The morphology of SWCNT layer and SWCNT-Al bilayer was observed by a field-emission scanning electron microscopy (FESEM, JSM-7001, JEOL). The work function of  $\text{In}_2\text{O}_3$ , SWCNTs and Al were measured by surface analyzer photoelectron spectrometer (AC-2, Riken Keiki Co. Ltd) at an amount of irradiation with light of 500 nW. The electrical properties of SWCNT and SWCNT-Al bilayer electrode TFTs were estimated by a semiconductor parameter analyzer (Agilent B1500A, Agilent Technologies) at room temperature.

## Results and discussion

Fig. 1b and c are top view SEM images of the SWCNT layer and the SWCNT/7 nm-thick Al bilayer films on  $\text{In}_2\text{O}_3$ . SWCNTs were deposited on a substrate characterized by an intrinsic random network, providing a percolating path for the carrier transport. However, the effective contact area of the SWCNTs with the  $\text{In}_2\text{O}_3$  thin film was smaller than originally planned, due to the presence of non-contact region, highlighted by the red circle in Fig. 1b. In case of the SWCNT-Al bilayer film, the effective contact area of the electrodes was the same as that of the originally planned electrodes. Fig. 1c shows the typical morphology of the SWCNT-Al bilayer. An island-type growth of the 7 nm Al film fully covered the substrate, as clearly observed through the open spaces of SWCNT layer covering it. Fig. 2a shows the energy band diagrams of the SWCNT electrodes/ $\text{In}_2\text{O}_3$  channel layer and of the SWCNT-Al bilayer electrodes/ $\text{In}_2\text{O}_3$  channel layer junctions. The work functions of  $\text{In}_2\text{O}_3$ , SWCNTs and Al are 4.50, 4.95 and 4.28 eV, respectively, as measured by surface analyzer. The carrier injection barrier of 0.45 eV from SWCNT to  $\text{In}_2\text{O}_3$  could be reduced by 0.22 eV when the Al layer was inserted. Moreover, in case of p-type semiconductor channel layer, novel metals such as gold, silver and copper having a high work function should be inserted to form the Ohmic contact because the work function of SWCNT is near the middle of Fermi energy of typical n-type and p-type semiconductor.

As shown in Fig. 2b, the structure of the SWCNT-Al bilayer/ $\text{In}_2\text{O}_3$ /heavily doped p-type Si substrate with a thermally oxidized 300 nm thick  $\text{SiO}_2$  layer was fabricated to examine the current-voltage characteristics of the

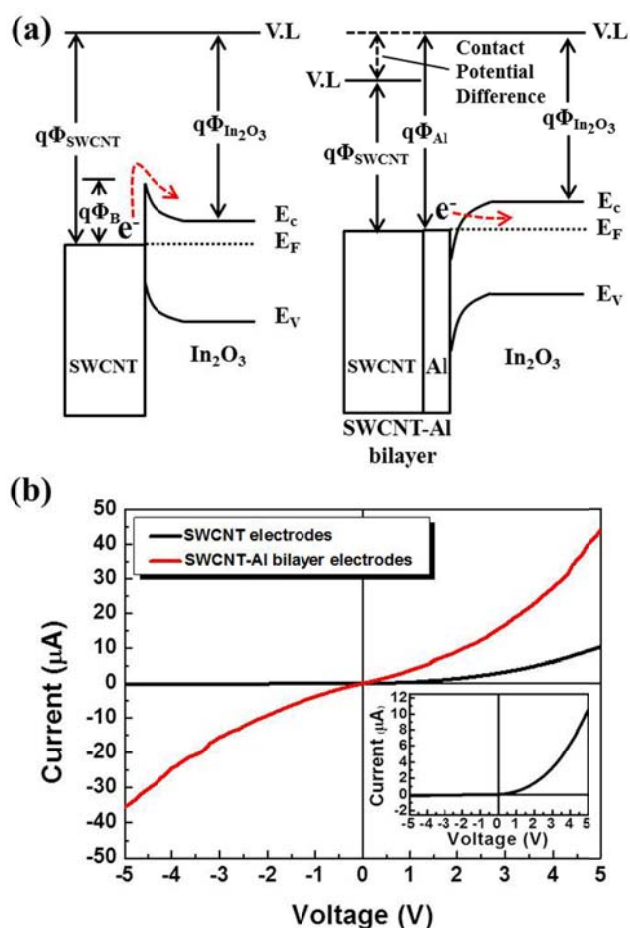


**Fig. 2** (a) Band diagrams of junctions between SWCNT electrodes and In<sub>2</sub>O<sub>3</sub> channel layer and between SWCNT-Al bilayer and In<sub>2</sub>O<sub>3</sub> channel layer, respectively. (b) The I-V characteristics of SWCNT/In<sub>2</sub>O<sub>3</sub> (black line) and SWCNT-7nm-thick Al bilayer/In<sub>2</sub>O<sub>3</sub> (red line).

SWCNT/In<sub>2</sub>O<sub>3</sub> and SWCNT/7 nm-thick Al bilayer/In<sub>2</sub>O<sub>3</sub> electrical junctions.

The current-voltage characteristic of the SWCNT/In<sub>2</sub>O<sub>3</sub> coincided with that of a typical Schottky diode and the current value of the In<sub>2</sub>O<sub>3</sub> channel layer was ~10 μA at 5 V. In contrast, the current-voltage characteristics of the SWCNT-Al bilayer showed an Ohmic behaviour and the current increased to ~50 μA at 5 V, as shown in Fig. 2b. Figure S1 shows the current-voltage characteristics of the SWCNT-Al bilayer as a function of the Al thickness (0, 5, 7 and 9 nm, respectively). The current dramatically increased up to ~7 mA at 5 V in case of a 9 nm-thick Al layer, indicating that the Al layer led to a significant reduction of the contact resistance between the electrodes and the In<sub>2</sub>O<sub>3</sub>.

The reduction of the contact resistance in the SWCNT-Al bilayer electrodes was investigated by using the transmission line method (TLM). We fabricated the SWCNT-Al bilayer/In<sub>2</sub>O<sub>3</sub>/SiO<sub>2</sub>/p<sup>++</sup>-Si and the SWCNT/In<sub>2</sub>O<sub>3</sub>/SiO<sub>2</sub>/p<sup>++</sup>-Si. The configurations of TLM devices are the same as those of the TFTs. The channel width of TLM patterns was 400 μm and the channel length was varied from 50 to 250 μm, while the gate voltage was modulated from 5 to 20 V. Fig. 3a and c show the

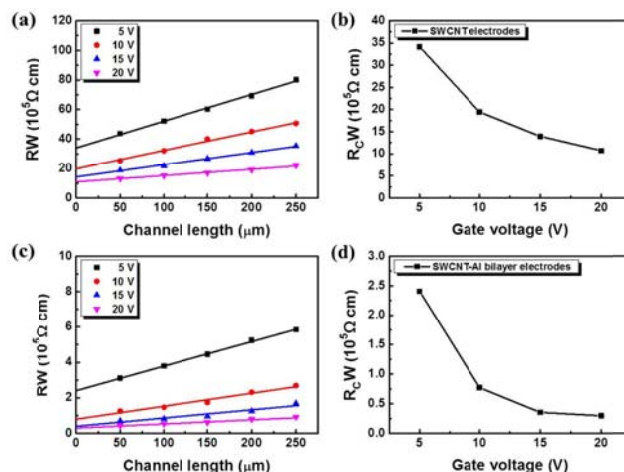


**Fig. 3** Width normalized resistance (RW) as a function of channel length with different gate voltages ( $V_{GS}$ ) from 5 to 20 V for (a) SWCNT and (c) SWCNT-Al bilayer electrode TFTs. Width normalized contact resistance ( $R_{CW}$ ) for (b) SWCNT and (d) SWCNT-Al bilayer electrode TFTs with various gate voltages.

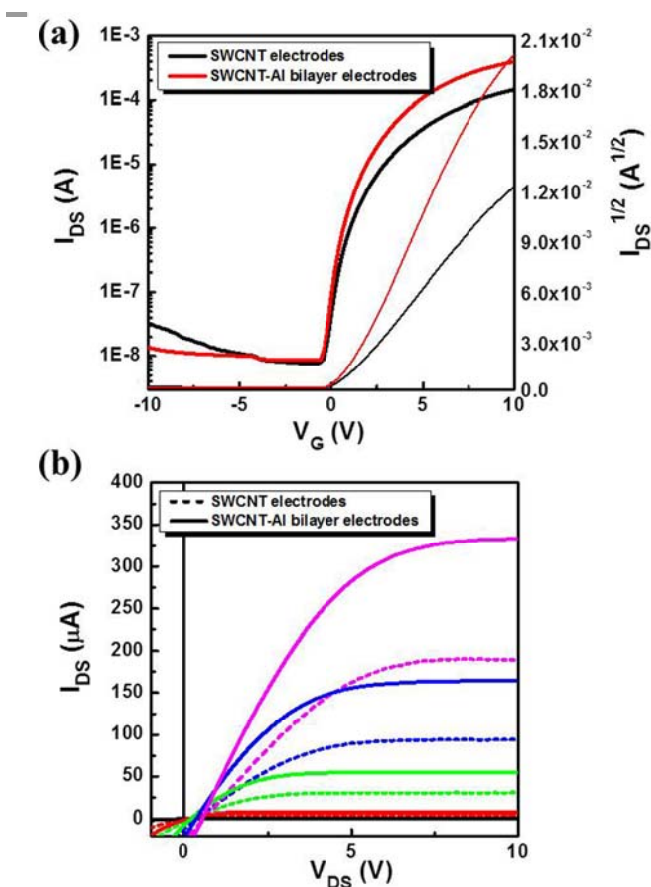
width normalized resistance (RW) of the channel length, given by the sum of the intrinsic channel resistance ( $R_{ch}$ ) and the contact resistance ( $R_{CW}$ ), depending on the gate voltage. The  $R_{CW}$  was calculated from the intersection of RW at  $L=0$  for each gate voltage.<sup>27,28</sup> For the SWCNT electrode TFT, the  $R_{CW}$  changed from 3.4 to 1.25 MΩ with increasing the gate voltage from 5 to 20 V, as shown in Fig. 3b.

The  $R_{CW}$  value for the SWCNT-Al bilayer electrode TFT changed from 240.8 to 29.6 KΩ with increasing the gate voltage, as shown in Fig. 3d. The SWCNT electrode TFT presents a higher  $R_{CW}$  than the SWCNT-Al bilayer electrode TFT. The  $R_{CW}$ s corresponding to different thicknesses of the Al layer are shown in Fig. S2.  $R_{CW}$ s varied from 99.6 to 498.3 KΩ for the SWCNT/5 nm-thick Al electrode TFT, and from 1.02 MΩ to 248.2 KΩ for the SWCNT/9 nm-thick Al electrode TFT. The contact resistance decreased as the thickness of the Al layer increased. However, if the Al layer was thicker than 9 nm, the contact resistance increased because of the damages caused on the electrodes during the long lift-off process.

In order to determine the effect of lowering the contact resistance due to the Al layer insertion on the device performance, we fabricated a SWCNT-Al bilayer/In<sub>2</sub>O<sub>3</sub>/HfO<sub>2</sub>/ITO glass bottom gate, top contact TFT. The thickness of the SWCNTs, Al, In<sub>2</sub>O<sub>3</sub> and HfO<sub>2</sub> layers were 100, 7, 15 and 50 nm, respectively. The source and drain electrodes had the channel width and length of 150 and 20 μm, a  $V_{th}$  of 0.66 V, a  $\mu_e$  of 1.59 cm<sup>2</sup>/V·s and an on/off current ratio ( $I_{on}/I_{off}$ ) of 3.12 × 10<sup>5</sup> at a  $V_D$  of 5 V, whereas the SWCNT/7 nm-thick Al electrode TFT had a  $S$  of 0.47 V/decade, a  $V_{th}$  of 0.45 V, a  $\mu_e$  of 4.50 cm<sup>2</sup>/V·s and an  $I_{on}/I_{off}$  of 6.86 × 10<sup>5</sup> at a  $V_D$  of 5 V. In addition, the electrical properties as a function of the Al layer thickness are shown in Fig. S3 and Table S1, indicating that the optimum thickness of the Al layer is 7 nm. The electrical properties of SWCNT and SWCNT-Al bilayer electrode TFTs and some literatures for the metal oxide TFTs with SWCNT electrode are summarized in Table 1. As a result,

**Table 1** Summarized electrical properties of SWCNT and SWCNT-Al bilayer electrode TFTs and some literatures for the metal oxide TFTs with SWCNT electrode

TFT Structure	Sub-threshold slope (V/decade)	Threshold voltage (V)	Field-effect mobility (cm <sup>2</sup> /V·s)	On/off current ratio	Ref.
SWCNT /In <sub>2</sub> O <sub>3</sub> /HfO <sub>2</sub> /ITO/Glass	0.66	0.66	1.59	3.12 × 10 <sup>5</sup>	
SWCNT-Al bilayer /In <sub>2</sub> O <sub>3</sub> /HfO <sub>2</sub> /ITO/Glass	0.47	0.45	4.50	6.86 × 10 <sup>5</sup>	
SWCNT /ZTO/Si <sub>3</sub> N <sub>4</sub> /ITO/Glass	1.4	15	1.3	1.02 × 10 <sup>7</sup>	24
SWCNT /IZO/ZAZ/ITO:F/Glass	0.735	2.92	0.45	1.01 × 10 <sup>6</sup>	25

**Fig. 4** Electrical properties of TFTs. (a) Transfer characteristics of SWCNT (black line) and SWCNT-Al bilayer (red line) electrode TFTs with a  $V_D$  of 5 V. (b) Output characteristics of SWCNT (dashed line) and SWCNT-Al bilayer (solid line) electrode TFTs with  $V_{GS}$  = 0 to 8 V in 2 V steps.

the SWCNT/7 nm-thick Al electrode TFT shows a performance by three times higher than that of the SWCNT electrode TFT. Also, our device showed superior electrical performance to other literature's results.

The reason for this enhancement in the device performance can be explained as following. (1) The High contact resistance makes more difficult the injection of carriers from the electrode to the semiconductor, with this carrier injecting ability being inversely proportional to the contact resistance. The Al inserting layer increases the effective contact area between the

electrodes and the active layer, so that the contact resistance of the TFT decreases. (2) Al presents a low work function, enabling a good Ohmic contact with In<sub>2</sub>O<sub>3</sub>. Fig S4 shows the optical transmittance spectra of the SWCNT and the SWCNT-Al bilayer electrode TFTs in visible range, and the optical image is shown in the inset of it. The transmittance was 72.22% for the SWCNTs electrode TFT and 70.82% for the SWCNTs-Al bilayer electrode TFT at 550 nm, respectively. Both devices exhibit similar transparency.

## Conclusions

In summary, the contact resistance has an important effect on the electrical characteristics of TFTs. We presented a study on the improvement of contact resistance between SWCNTs and In<sub>2</sub>O<sub>3</sub> based on a solution process. In order to reduce the high energy barrier for SWCNTs, we deposited Al as a contact layer between the SWCNTs and In<sub>2</sub>O<sub>3</sub> films. Due to the enlargement of the contact area between the channel layers and to the low work function of Al, both contact resistance and energy barrier were reduced. This indicates that the work function affects the contact resistance. An integrated device consisting of HfO<sub>2</sub>, In<sub>2</sub>O<sub>3</sub> and SWCNT-Al bilayers as gate insulator, channel layers and source/drain electrodes, respectively, was fabricated on ITO-deposited bottom gate glass. The process temperature was maintained under the 250 °C. The SWCNT-Al bilayer electrode TFT exhibited a threshold voltage of 0.45 V, a mobility of 4.50 cm<sup>2</sup>/V·s and an  $I_{on}/I_{off}$  of  $6.86 \times 10^5$ .

## Acknowledgements

This research was supported by the LG Display academic industrial cooperation program.

## Notes and references

<sup>a</sup> Department of Materials Science and Engineering, Yonsei University, 50 Yonsei-ro, Seodaemun-gu, Seoul 120-749, Korea. E-mail: jmmyoung@yonsei.ac.kr

<sup>b</sup> College of BioNano Technology, Gachon University, 1342 Seongnamdae-ro, Sujeong-gu, Seongnam-si, Gyeonggi-do 461-701, Korea.

<sup>c</sup> School of Electrical and Electronic Engineering, Yonsei University, 50 Yonsei-ro, Seodaemun-gu, Seoul 120-749, Korea.

<sup>d</sup> LG Display LCD Research and Development Center, 245 Lg-ro, Wollong-myeon, Paju-si, Gyeonggi-do 413-811, Korea.

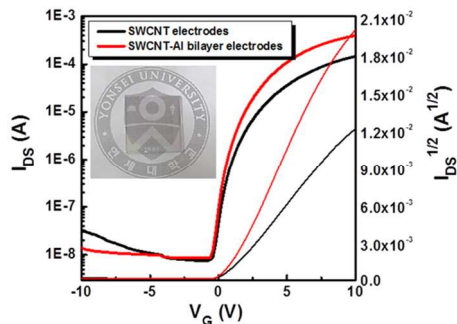
† Footnotes should appear here. These might include comments relevant to but not central to the matter under discussion, limited experimental and spectral data, and crystallographic data.

Electronic Supplementary Information (ESI) available: [Fig. S1 the current-voltage curves of the SWCNT-Al bilayer film with the Al thickness of none, 5, 7 and 9 nm. Fig. S2 the  $R_W$  and the  $R_CW$  as a function of channel length with different  $V_{GS}$  for the SWCNT/5 nm-thick Al bilayer and the SWCNT/9 nm-thick Al bilayer electrode TFTs. Fig. S3 I-V characteristics of the SWCNT/5 nm-thick Al bilayer and the SWCNT/9 nm-thick Al bilayer electrode TFTs. Table S1 summarized electrical properties of TFTs. Fig. S4 optical transmittance spectra of the SWCNT and the SWCNT-Al bilayer electrode TFTs.]. See DOI: 10.1039/b000000x/

‡ Su Jeong Lee and Tae Il Lee contributed equally to this work.

- 1 M.-G. Kim, M. G. Kanatzidis, A. Facchetti and T. J. Marks, *Nat. Mater.*, 2011, **10**, 382.
- 2 S. Y. Park, B. J. Kim, K. Kim, M. S. Kang, K.-H. Lim, T. I. Lee, J. M. Myoung, H. K. Baik, J. H. Cho and Y. S. Kim, *Adv. Mater.*, 2012, **24**, 834.
- 3 S. Jeong and J. Moon, *J. Mater. Chem.*, 2012, **22**, 1243.
- 4 K. M. Kim, C. W. Kim, J.-S. Heo, H. Na, J. E. Lee, C. B. Park, J.-U. Bae, C.-D. Kim, M. Jun, Y. K. Hwang, S. T. Meyers, A. Grenville and D. A. Keszler, *Appl. Phys. Lett.*, 2011, **99**, 242109-1.
- 5 S. R. Thomas, P. Pattanasattayavong and T. D. Anthopoulos, *Chem. Soc. Rev.*, 2013, **42**, 6910.
- 6 G. Adamopoulos, A. Bashir, W. P. Gillin, S. Georgakopoulos, M. Shkunov, M. A. Baklar, N. Stingelin, D. D. C. Bradley and T. D. Anthopoulos, *Adv. Funct. Mater.*, 2011, **21**, 525.
- 7 H. Faber, J. Hirschmann, M. Klaumünzer, B. Braunschweig, W. Peukert and M. Halik, *ACS Appl. Mater. Interfaces.*, 2012, **4**, 1693.
- 8 D. S. Hecht, L. Hu and G. Irvin, *Adv. Mater.*, 2011, **23**, 1482.
- 9 X. Huang, Z. Zeng, Z. Fan, J. Liu, and H. Zhang, *Adv. Mater.*, 2012, **24**, 5979.
- 10 A. R. Rathmell, S. M. Bergin, Y.-L. Hua, Z.-Y. Li and B. J. Wiley, *Adv. Mater.*, 2010, **22**, 3558.
- 11 H. Wu, L. Hu, T. Carney, Z. Ruan, D. Kong, Z. Yu, Y. Yao, J. J. Cha, J. Zhu, S. Fan and Y. Cui, *J. Am. Chem. Soc.*, 2011, **133**, 27.
- 12 Z. Yu, Q. Zhang, L. Li, Q. Chen, X. Niu, J. Liu and Q. Pei, *Adv. Mater.*, 2011, **23**, 664.
- 13 D. Langley, G. Giusti, C. Mayousse, C. Celle, D. Bellet and J.-P. Simonato, *Nanotechnology.*, 2013, **24**, 452001-1.
- 14 G. Gruner, *J. Mater. Chem.*, 2006, **16**, 3533.
- 15 H. Park, J.-S. Kim, B. G. Choi, S. M. Jo, D. Y. Kim, W. H. Hong and S.-Y. Jang, *Carbon.*, 2010, **48**, 1325.
- 16 L. Hu, H. Wu and Y. Cui, *MRS Bull.*, 2011, **36**, 760.
- 17 A. Kim, Y. Won, K. Woo, C. H. Kim and J. Moon, *ACS Nano.*, 2013, **7**, 1081.
- 18 H. H. Khaligh and I. A. Goldthorpe, *Nanoscale Res. Lett.*, 2013, **8**, 235.
- 19 J.-Y. Lee, S. T. Connor, Y. Cui and P. Peumans, *Nano Lett.*, 2008, **8**, 689.
- 20 R. L. McCreery, *Chem. Rev.*, 2008, **108**, 2646.
- 21 I. Dumitrescu, P. R. Unwin and J. V. Macpherson, *Chem. Commun.*, 2009, **45**, 6886.
- 22 M. Pumera, *Chem. Eur. J.*, 2009, **15**, 4970.
- 23 D. K. Singh, P. K. Iyer and P. K. Giri, *J. Appl. Phys.*, 2010, **108**, 084313-1.
- 24 J. Jeon, T. I. Lee, J. H. Choi, J. P. Kar, W. J. Choi, H. K. Baik and J. M. Myoung, *Electrochem. Solid-State Lett.*, 2011, **14**, H76.
- 25 J. H. Park, S. J. Lee, T. I. Lee, J. H. Kim, C. H. Kim, G. S. Chae, M. H. Ham, H. K. Baik and J. M. Myoung, *J. Mater. Chem. C*, 2013, **1**, 1840.
- 26 J. H. Park, Y. B. Yoo, K. H. Lee, W. S. Jang, J. Y. Oh, S. S. Chae, H. W. Lee, S. W. Han and H. K. Baik, *ACS Appl. Mater. Interfaces.*, 2013, **5**, 8067.
- 27 Y. Jung, T. Jun, A. Kim, K. Song, T. H. Yeo and J. Moon, *J. Mater. Chem.*, 2011, **21**, 11879.
- 28 G. B. Blanchet, C. R. Fincher, M. Lefenfeld and J. A. Rogers, *Appl. Phys. Lett.*, 2004, **84**, 296.
- 29 B. G. Streetman and S. Banerjee, *Solid State Electronic Devices 6th edn* (Upper Saddle River, NJ: Pearson Education), 2006.

## Graphical abstract



The Electrical properties of TFTs. The transfer characteristics of the SWCNT and SWCNT-Al bilayer electrode TFTs on ITO coated glass substrate with  $HfO_2$  gate dielectric and  $In_2O_3$  Channel layer. The inset shows optical image of the SWCNT-Al bilayer electrode TFT.